Taylor & Francis
Taylor & Francis Group

Pharmaceutical Development and Technology

ISSN: (Print) (Online) Journal homepage: https://www.tandfonline.com/loi/iphd20

Compression–decompression modulus (CDM) – an alternative/complementary approach to Heckel's analysis

Devang B. Patel, Vivek D. Patel, Yash Patel, John C. Sturgis, Robert Sedlock & Rahul V. Haware

To cite this article: Devang B. Patel, Vivek D. Patel, Yash Patel, John C. Sturgis, Robert Sedlock & Rahul V. Haware (2022): Compression–decompression modulus (CDM) – an alternative/complementary approach to Heckel's analysis, Pharmaceutical Development and Technology, DOI: 10.1080/10837450.2022.2120895

To link to this article: https://doi.org/10.1080/10837450.2022.2120895

PHARMACEUTICAL DEVELOPMENT AND TECHNOLOGY
https://doi.org/10.1080/10837450.2022.2120895

Taylor & Francis
Taylor & Francis Group

RESEARCH ARTICLE

Compression–decompression modulus (CDM) – an alternative/complementary approach to Heckel's analysis

Devang B. Patel[a], Vivek D. Patel[a], Yash Patel[b], John C. Sturgis[a], Robert Sedlock[a] and Rahul V. Haware[a]

[a]Natoli Scientific, A Division of Natoli Engineering Company, Inc., Telford, PA, USA; [b]Sharp Clinical Services, LLC, Bethlehem, PA, USA

ABSTRACT

The novel modulus-based approach was developed to characterize the compression behavior of the materials and how it results into tablet mechanical strength (TMS) of the final tablet. The force–displacement profile for the model materials (Vivapur® 101, Starch 1500®, Emcompress®, and Tablettose® 100) was generated at different compression pressures (100, 150, and 200 MPa) and speeds (0.35, 0.55, and 0.75 m/s) using compaction emulator (Presster™). A generated continuous compression profile was evaluated with Heckel plot and the proposed material modulus method. The computed compression parameters were qualitatively and quantitatively correlated with TMS by principal component analysis and principal component regression, respectively. Compression modulus has negatively correlated, while decompression modulus is positively correlated to TMS. Proposed modulus descriptors are independent of particle density measurements required for the Heckel method and could overcome the limitations of the Heckel method to evaluate the decompression phase. Based on the outcome of the study, a two-dimensional compression and decompression modulus classification system (CDMCS) was proposed. The proposed CDMCS could be used to define critical material attributes in the early development stage or to understand reasons for tablet failure in the late development stage.

ARTICLE HISTORY
Received 29 April 2022
Revised 16 August 2022
Accepted 31 August 2022

KEYWORDS
Compression modulus; decompression modulus; Heckel's analysis; deforming materials; fragmenting materials

1. Introduction

The compression profiles parameterization generated with a few grams of pharmaceutical materials using the compaction simulator serves as an important baseline information for the timely development of robust tablet formulations. Baseline information could be relayed in defining the critical material attributes (CMAs) of the formulation component. CMAs are an important cog of subsequent risk-assessment associated with the potential formulation even before the phase-I stage. Active pharmaceutical ingredients (APIs) are mainly poorly compressible under applied compression pressure. In this case, it is necessary to add other excipients to make the final API formulation compressible enough to produce the robust tablet. It is important to understand the material's intrinsic deformation or fragmentation tendencies under the applied compression load as it may dominate the properties of final tablets. Compression profiling of API and selected excipients could serve as a powerful knowledge tool in these scenarios to make a smart selection of excipients to generate confidence in the developed prototype formulation in the very early development stage. An early introduction of compaction simulation and subsequent compression profile parameterization with a suitable mathematical modeling in the product development stage could establish a solid base for knowledge-based decisions in such critical formulation issues.

Currently, Heckel's method has gained wider application to parameterize compression profiles to evaluate the macroscopic compression properties of the pharmaceutical materials. Heckel's method is based on the measured powder particle density in addition to its sensitivity to the experimental conditions (Rue and Rees 1978; Sonnergaard 1999). The powder particle density measured at zero compression pressure is not a true reflection of the 'at-pressure' powder particle density (Patel et al. 2022). It has also been previously reported that a small error (1%) in the powder particle density leads to 10.0% of relative error in the porosity (Sonnergaard 1999). These errors are significantly impacting the values of derived Heckel's descriptors. Heckel's analysis is also prone to a negative porosity issue in the high-pressure regions (Patel et al. 2022). A Heckel plot with high-pressure negative porosities is devoid of the entire decompression phase. The loss of the decompression phase in the Heckel plot is a possible squander of important information about the elastic behavior of the materials. It is vital information for understanding the potential tableting problems like capping and lamination.

An alternative way of understanding material deformation and fragmentation properties has been proposed and evaluated in this present study to eclipse above-mentioned limitations of the Heckel analysis. This approach includes an estimation of the material modulus. The material modulus in the compression and decompression phases could be calculated by parameterizing the force–displacement data obtained with the compaction simulator into a strain and stress relationship. The modulus calculated with force–displacement data from the compression and decompression phase is called as a compression and decompression modulus (CDM), respectively. As these moduli calculations are not using the powder particle density, they could be immune to the limitations associated with the Heckel analysis.

CONTACT Rahul V. Haware rhaware@natoli.com Natoli Scientific, A Division of Natoli Engineering Company, Inc., 100 Emlen Way, Suite # 104-108, Telford, PA 18969, USA

Supplemental data for this article can be accessed online at https://doi.org/10.1080/10837450.2022.2120895

Thus, the present investigation aimed to evaluate the generated dynamic compression profile using the compaction simulator with proposed compression and decompression modulus (CDM) methods. Various model materials such as Vivapur® 101, Starch 1500®, Emcompress®, and Tablettose® 100 were selected to represent the predominantly plastic, elastic, high fragmenting, and low fragmenting material compression behaviors, respectively. These materials were compressed at three different compression pressures (100, 150, and 200 MPa) and three different linear compression speeds (0.35, 0.55, and 0.75 m/s). The compression profile was also evaluated with the '*in-die*' Heckel method. The generated data set was evaluated qualitatively and quantitatively by multivariate methods to understand the compliance of proposed modulus descriptors and Heckel's descriptors with tablet mechanical strength (TMS). Finally, computed CDM were used to propose a two-dimensional compression–decompression modulus classification system (CDMCS). The proposed CDM methodology and classification system is a 'proof of concept' of our series of studies. The future studies will be focusing on the binary powder and actual formulation systems. These studies are not within the scope of the present report. The proposed CDMCS could be used for defining CMAs in the early development stage or to understand possible reasons for tablet failure in the late development stage.

2. Materials

Vivapur® 101 (microcrystalline cellulose, lot no. V101C20G62, JRS Pharma LP, Patterson, NY), Starch 1500® (partially pregelatinized maize starch, lot no. IN544252, Colorcon Inc., West Point, PA), Emcompress® (dibasic calcium phosphate dihydrate, lot no. 837551X, JRS Pharma LP, Patterson, NY), and Tablettose® 100 (α-lactose monohydrate, lot no. L104294020, Meggle Pharma, Wasserburg, Germany) were used as model materials to represent predominantly plastic, elastic, high fragmenting, and low fragmenting behaviors, respectively, in this study. All materials were used as received.

3. Methods

3.1. Particle density measurement

The powder particle density of each material was determined using a helium displacement pycnometer (AccuPyc™ II 1340, Micromeritics GmbH, Neuss, Germany). A stainless-steel chamber with volume of 10 cm^3 was installed in helium displacement pycnometer. The volume of sample holder was 3.5 cm^3. A powder weight required to fill 3/4th volume of sample holder was weighed on an analytical balance (model EBL 164e, Adam Equipment, Oxford, CT). The powder was purged with five repetitive cycles before measuring the powder particle density in triplicate. The mean of these measurements was taken as the powder particle density.

3.2. Experimental design for dynamic compression profiles

Continuous dynamic compression profiles of each material were generated using a compaction emulator (Presster™, Natoli Scientific, Telford, PA) emulating the Natoli NP-400 tablet press (28 stations). The compaction emulator was set up with 250 mm diameter compaction rolls and a round 10 mm diameter flat-faced 'B' tableting specification manual (TSM) domed tool to compress each material. The powder was compressed at a compression pressure of 100, 150, and 200 MPa and a linear compression speed of 0.35, 0.55, and 0.75 m/s. Tablet weight of Vivapur® 101 was 300 mg, Starch 1500® was 287 mg, Emcompress® was 440 mg, and Tablettose® 100 was 295 mg. Tablet weight was calculated with a theoretical constant particle volume of $0.1911 \pm 0.0005\ cm^3$. The constant particle volume was used to determine the theoretical tablet weight to mimic the volumetric die filling of typical industrial tablet manufacturing (Çelik and Okutgen 1993). A manually weighed and fed powder was compressed at the above-mentioned compression parameters. The inner wall of the die, upper punch tip, and lower punch tip were externally lubricated with magnesium stearate slurry (1%w/v in acetone) before each compression. Tablet weight was measured immediately after ejection from the die. The tablets were stored for 24 h before measuring tablet dimensions (thickness and diameter) and breaking force. Tablet mechanical strength (MPa) was calculated using the following equation (Fell and Newton 1970):

$$\mathrm{TMS} = \frac{2F}{\pi \mathrm{Dt}} \tag{1}$$

where F is the breaking force (N), D is the diameter (mm), and t is the thickness (mm).

3.3. Heckel parameterization of compression profiles

A generated dynamic compression profile at different experimental conditions was parameterized with '*in-die*' Heckel's method (Equation (2)) (Heckel 1961a, 1961b):

$$\ln\left[\frac{1}{1-D}\right] = kP + A \tag{2}$$

where D is the relative density of the compacted powder at applied compression pressure P (MPa), and A is the Y-intercept. The ln [1/1 – D] is determined using the powder particle density and '*in-die*' compact thickness. The reciprocal slope of compression and decompression phases was used to compute yield pressure (YP) of plastic deformation (YPpl) and yield pressure of elastic recovery (YPel) values, respectively. The YPpl and YPel were computed using linear regions of the Heckel plot from the compression and decompression phase, respectively. The unit of these parameters was MPa. The linear regions were determined by performing a regression analysis. The linear regions of compression and decompression pressure with R^2 value >0.95 were used to compute Heckel's YP values. The linear ranges of compression and decompression phase used for Heckel's parameterization after compressing model material powders at different compression pressures were as follows: compression pressure 100 MPa:20–80 MPa; compression pressure 150 MPa:20–130 MPa; compression pressure 200 MPa:20–180 MPa.

3.4. Apparent work of compression

The apparent work of compression (WoC) was determined from the force–displacement data using the following equation (Ragnarsson 1996):

$$\mathrm{WoC} = \int_0^{D_{\max}} F.dD - \int_{D_T}^{D_{\max}} F.dD \tag{3}$$

where F is the applied compression force (N), D_{max} is the compact thickness at applied maximum compression force (mm), and D_T is the 'in-die' compact thickness at zero decompression force (mm). The compression force range used in the present study for integrating WoC was from 0 to 7850 N (~100 MPa compression

pressure), 0 to 11775 N (~150 MPa compression pressure), and 0 to 15700 N (~200 MPa compression pressure).

3.5. Determination of compression–decompression modulus

Compression modulus and decompression modulus can be determined from the stress vs. strain plot. The compression and decompression stresses were calculated with applied compression and decompression forces and tooling dimensions to make compacts:

$$\text{Compression stress (MPa)} = \frac{F_C}{A} \quad (4)$$

$$\text{Decompression stress (MPa)} = \frac{F_d}{A} \quad (5)$$

where F_C is the applied compression force (N), A is the cross-sectional area of the punch tip (mm^2), and F_d is the decompression force (N).

The compression and decompression strain were estimated using the following equations:

$$\text{Compression strain} = \frac{IDT_{0C} - IDT_F}{IDT_{0C}} \quad (6)$$

$$\text{Decompression strain} = \frac{IDT_{0D} - IDT_F}{IDT_{0D}} \quad (7)$$

where IDT_{0C} is the '*in-die*' powder thickness (mm) at zero compression force, IDT_F is the '*in-die*' powder thickness (mm) at highest compression force, and IDT_{0D} is the '*in-die*' powder thickness (mm) after complete unloading of the compression force. The '*in-die*' powder thickness values at respective compression and decompression forces were collected from the force–displacement data recorded during each compression cycle. 'In-die' thickness data were not corrected during the data analysis. The impact of mechanical compliance on punch deformation under compression pressure is not relevant for these measurements due to the fixturing of the linear variable differential transducers (LVDTs) used to measure punch displacement. A stress vs. strain plot from 5 to 60 MPa compression pressure exhibited 'bi-linear' regions between 5–20 MPa and 20–60 MPa compression pressure (Figure 1(A)). These regions could indicate low pressure particle fragmentation followed by material deformation. Therefore, a plot of stress vs. strain was graphed in the low compression pressure range (5–20 MPa) and mid compression pressure range (20–60 MPa) for the compression and decompression phase of each material. These pressure ranges were selected based on their 'goodness-of-fit' for exhibited linearity. The portion of the plot having linear regression with $R^2 \geq 0.97$ was selected to indicate elastic region of modulus.

The slope of linear line equation (Equation (8)) exhibited the respective compression or decompression modulus.

$$\text{Stress (MPa)}(y) = \text{slope (m)} \times \text{strain (x)} + \text{Intercept (c)} \quad (8)$$

A slope of low and mid compression pressure range in the compression phase is defined as the compression modulus (CM) (Figure 1(B)). A slope of low and mid compression pressure range in the decompression phase is defined as the decompression modulus (DM) (Figure 1(C)).

3.6. Multivariate statistical analysis

A multivariate statistical analysis was performed using Unscrambler® v10 software (CAMO Software AS, Trondheim, Norway). A qualitative principal component analysis (PCA) and a quantitative principal component regression (PCR) analysis was

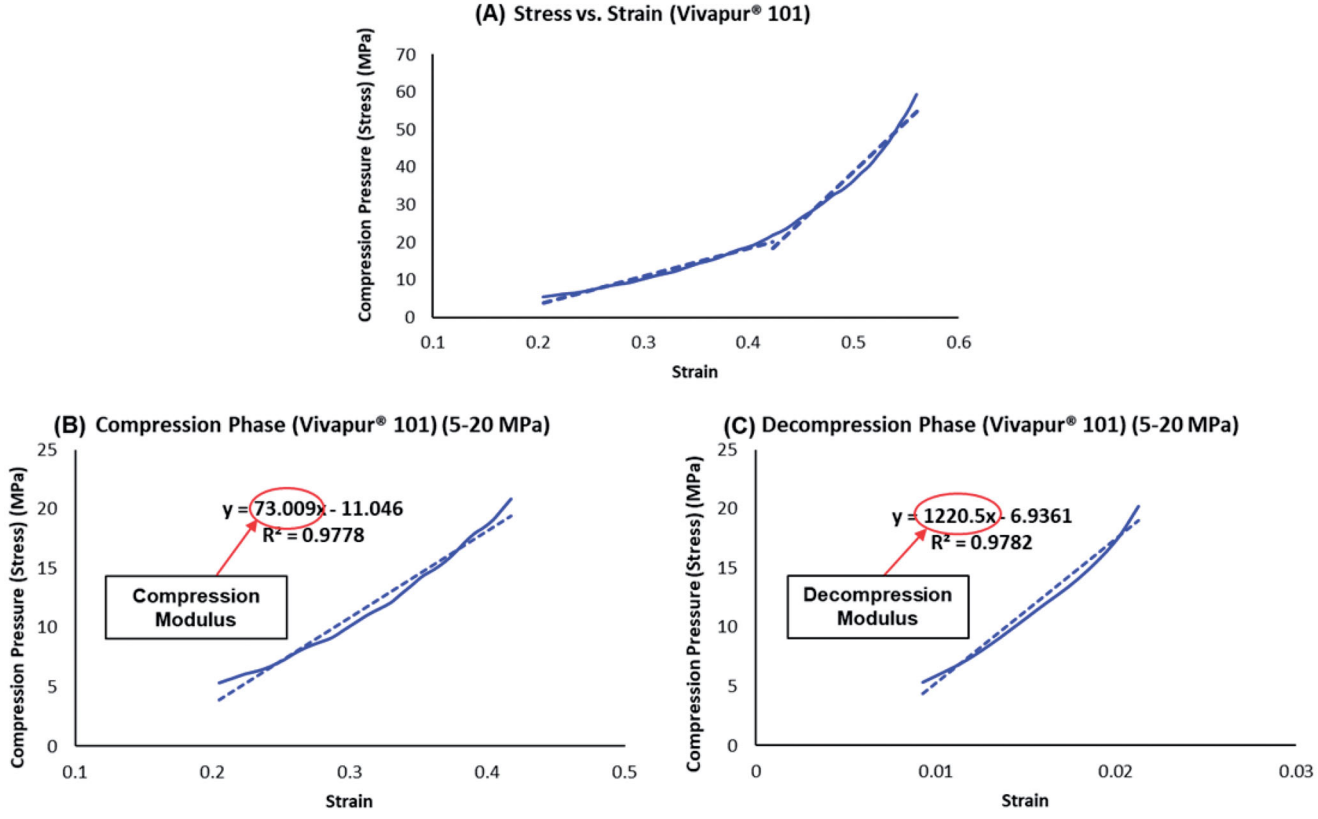

Figure 1. (A) Stress vs. strain plot of Vivapur® 101 in the range of 5–60 MPa compression pressure representing 'bi-linear' regions between 5–20 MPa and 20–60 MPa compression pressure. (B) Compression modulus in compression phase of 5–20 MPa. (C) Decompression modulus in the decompression phase of 5–20 MPa.

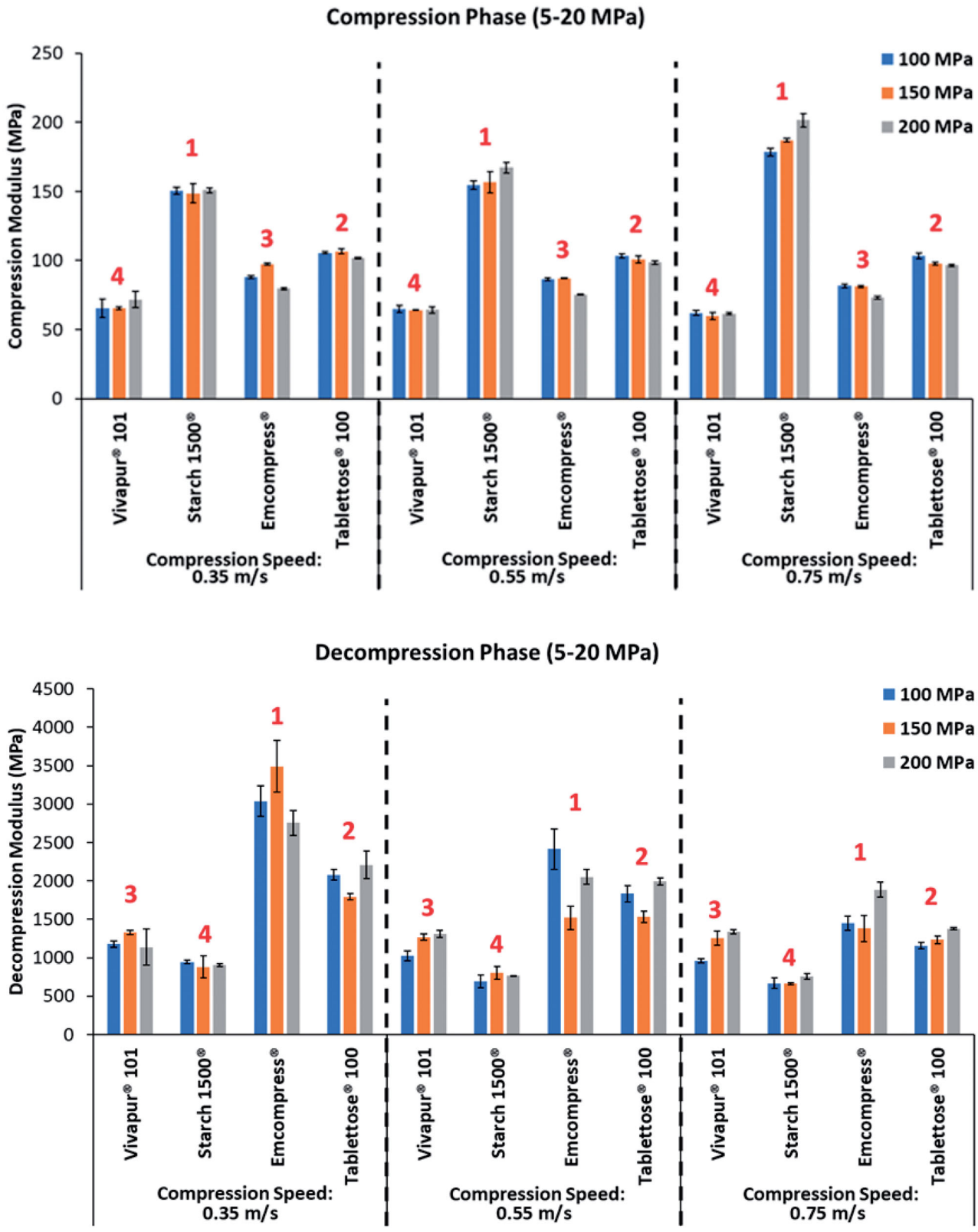

Figure 2. Compression and decompression modulus at low compression and decompression pressure range (5–20 MPa) for Vivapur® 101, Starch 1500®, Emcompress®, and Tablettose® 100 at a compression pressure of 100, 150, and 200 MPa and speed of 0.35, 0.55, and 0.75 m/s. Numbers (1–4) indicate the rank order of the material under each compression conditions.

used to evaluate the data set. All variables were weighed and scaled by dividing them with their standard deviation to avoid the undue influence of variable experimental range on the model outcome. *X*-variables considered in the PCA were CM, decompression modulus, YPpl, YPel, WoC, and TMS. A quantitative PCR was used to quantify statistically significant and insignificant contributions of the main effects of various *X*-variables. The *X*-variables used in this analysis were material type, compression

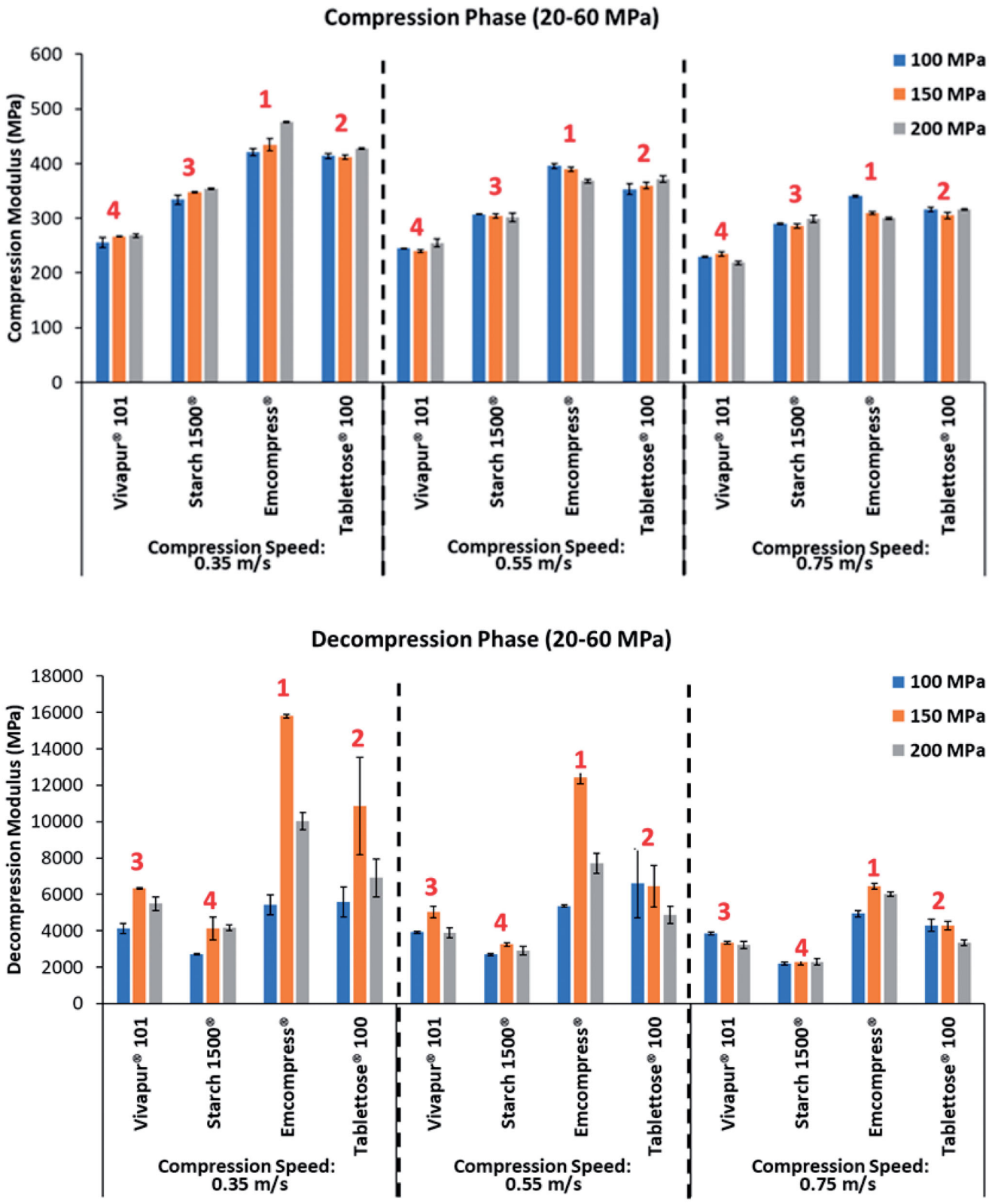

Figure 3. Compression and decompression modulus at mid compression and decompression pressure range (20–60 MPa) for Vivapur® 101, Starch 1500®, Emcompress®, and Tablettose® 100 at a compression pressure of 100, 150, and 200 MPa and speed of 0.35, 0.55, and 0.75 m/s. Numbers (1–4) indicate the rank order of the material under each compression conditions.

pressure, compression speed, CM, decompression modulus, WoC, and yield pressures (YPpl and YPel). The *Y*-variable was the TMS. Each material was coded as 0 and 1. These coded variables were split to separate the individual effect of each material on the TMS. The *X* and *Y* variables were initially weighted by dividing with their respective standard deviation before each modeling to give an equal weighting to each variable. The models were validated with a full cross-validation and the Jack-Knifing method (Martens and Martens 2000). The statistical significance of the model was measured at $\alpha < 0.05$.

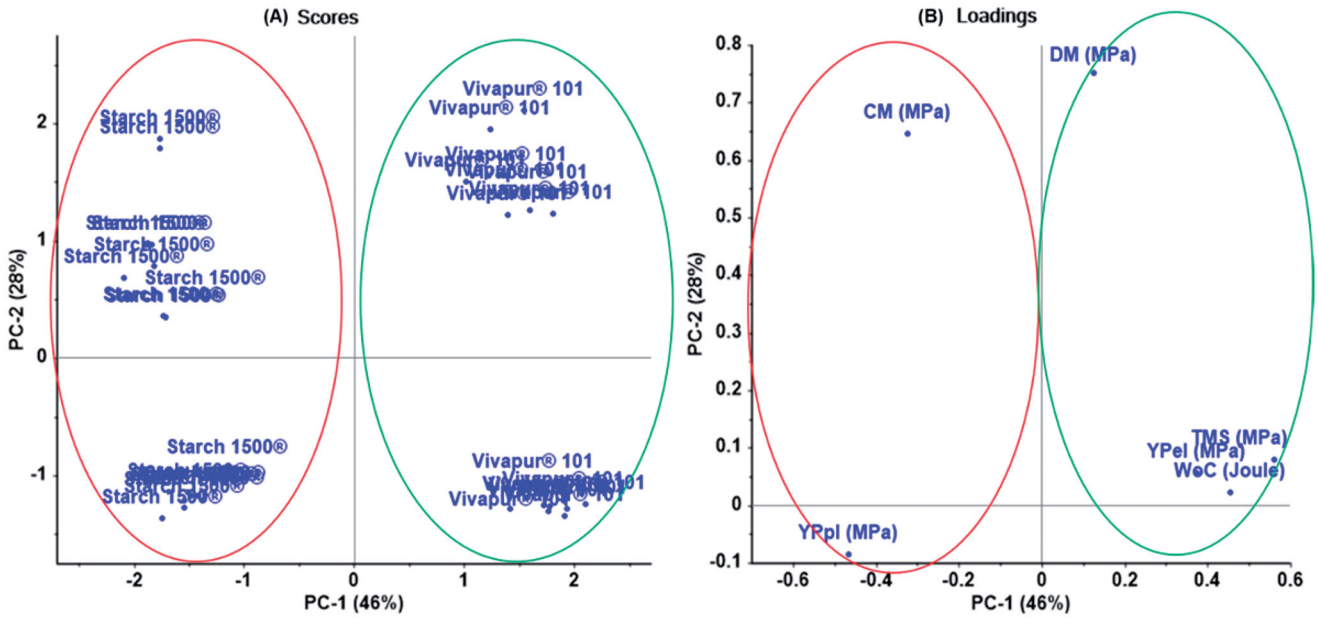

Figure 4. The principal component analysis (A) scores plot and (B) loadings plot of deforming materials; Vivapur® 101 and Starch 1500®, and their material properties. The first two principal components represent 74% of the variance in the data.

4. Results and discussion

4.1. Material's modulus

The CDM can provide insights into the material deformation, fragmentation, and elasticity under the applied and released compression load. Such derived material's modulus will serve as an indicator for differentiating material's characteristic during the tableting process. Table S1 (Supplementary Table) displays the CDM of the selected representative predominantly plastic (Vivapur® 101) (David and Augsburger 1977; Choi et al. 2010; Haware et al. 2010), elastic (Starch 1500®) (Paronen 1986; Choi et al. 2010), low fragmenting (Tablettose® 100) (De Boer et al. 1986; Haware et al. 2009a), and high fragmenting (Emcompress®) (Paronen 1986; Haware et al. 2009a) materials evaluated in the different compression pressure ranges and at different speeds. The CM of these materials in the low (5–20 MPa) (Figure 2) and mid (20–60 MPa) (Figure 3) compression pressure range was found in the following descending order:

$$\text{Starch 1500}^{®} > \text{Tablettose}^{®}\ 100 > \text{Emcompress}^{®} > \text{Vivapur}^{®}\ 101 (5-20\ \text{MPa})$$

$$\text{Emcompress}^{®} > \text{Tablettose}^{®}\ 100 > \text{Starch 1500}^{®} > \text{Vivapur}^{®}\ 101 (20-60\ \text{MPa})$$

The decompression modulus of these materials in the low (5–20 MPa) (Figure 2) and mid (20–60 MPa) (Figure 3) compression pressure range followed the same descending order:

$$\text{Emcompress}^{®} > \text{Tablettose}^{®}\ 100 > \text{Vivapur}^{®}\ 101 > \text{Starch 1500}^{®} (5-20\ \text{MPa and}\ 20-60\ \text{MPa})$$

This order of CDM was observed irrespective of the applied compression speed and pressure. The data presented in Supplementary Table S1 indicate that there is no effect of compression speed on observed CM and DM at applied compression condition. CM and DM mainly calculated from stress–strain plot. Compression speed does not affect the amount of stress applied and the amount of displacement happens under the applied compression pressure. It indicates that compression speed does not affect CM and DM of the material. A consistent order of moduli confirmed that evaluated moduli are characteristics of the differently deforming and fragmenting materials despite the applied compression conditions. The TMS of these materials was found in the following order.

$$\text{Vivapur}^{®}\ 101 > \text{Emcompress}^{®} \geq \text{Tablettose}^{®}\ 100 > \text{Starch 1500}^{®}$$

A predominantly elastic material exhibited high CM in the low compression pressure range as compared to other materials. It reflects their lower consolidation tendency by particle rearrangement and packing event as compared to other materials at lower compression pressure. It also revealed a high CM and a low decompression modulus as compared to the predominantly plastic material. A high compression and a low decompression modulus of Starch 1500® is an indication of a respective low and high strain or displacement in the compression and decompression phases. This can lead to a high material elasticity with weaker tableting. A predominantly plastic Vivapur® 101 presented exactly opposite CDM than elastic Starch 1500®. A high displacement followed by a low displacement in the respective compression and decompression phase could indicate the ability of plastic material to preserve most of its bonding friendly permanent deformation even after unloading the applied compression pressure. This ability eventually translates into their stronger tableting performance. The fragmenting materials showed higher CDM in the mid-pressure range than the deforming materials (Akseli et al. 2009). A high fragmenting Emcompress® exhibited a low CM and a high decompression modulus than the low fragmenting Tablettose® 100. The higher moduli of fragmenting materials are due to their limited displacement or low strain in the loading and unloading of the compression pressure. Such stiff materials could mainly rely on the increasing bonding numbers by fragmentation into the smaller particles to provide a desired tablet strength (Nyström and Karehill 1996; Choi et al. 2010). Thus, it is interesting to decode the role of macroscopic material moduli properties into the final transaction of the TMS.

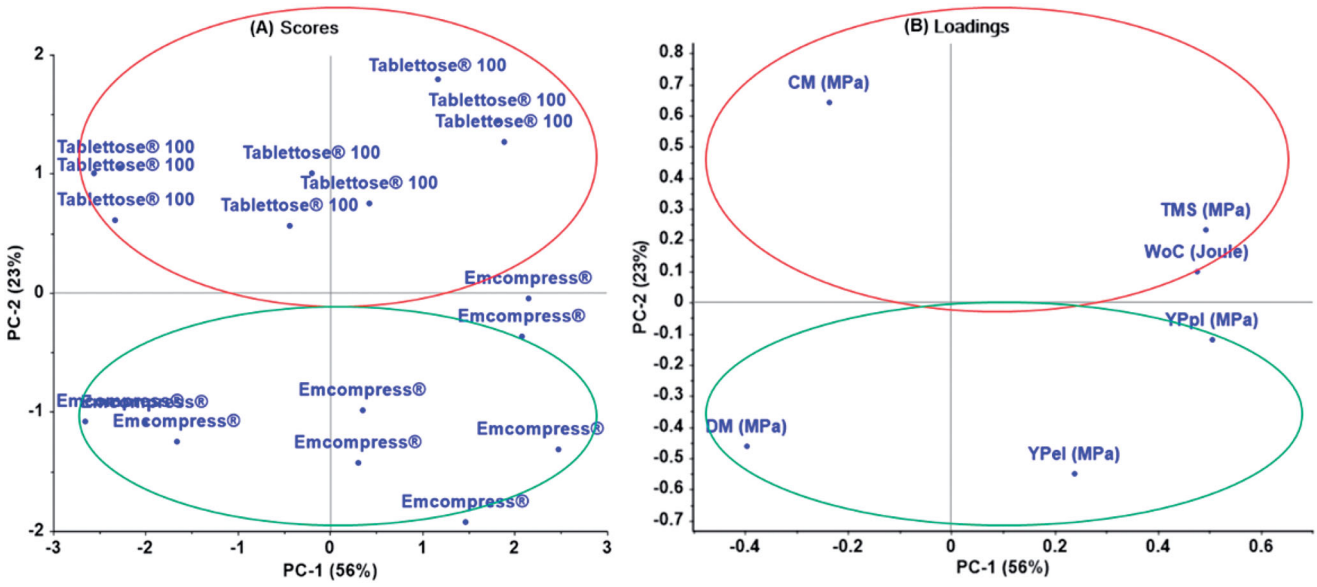

Figure 5. The principal component analysis (A) scores plot and (B) loadings plot of fragmenting materials; Emcompress®, and Tablettose® 100, and their material properties for the low compression and decompression pressure range (5–20 MPa). The first two principal components represent 79% of the variance in the data.

4.2. Qualitative quantification between material deformation properties and tablet mechanical strength

PCA was performed only on response variables. PCA score plot was used to exhibit distinct grouping related to differently deforming and fragmenting materials. PCA loadings plot was utilized to identify indicative dependent factors responsible for grouping. This PCA methodology was applied based on our previous experience (Haware et al. 2009a).

A two-step qualitative PCA was performed to decode the relationship between the evaluated material deformation properties by the CM, the decompression modulus, Heckel descriptors, and work descriptors with the TMS. A single PCA of deforming and fragmenting materials did not exhibit a separate grouping of these materials along the PC axis. Therefore, a separate PCA was performed with the deforming materials and fragmenting materials. This approach displayed expected separation of deforming and fragmenting materials along the PC axis. PCA scores plot decodes hidden groupings, similarities, or differences in the data structure. Samples and variables located on the same side of the principal component (PC) axis are positively correlated and vice-a-versa. PCA loadings plot provides the reasons behind the data decomposition observed in the PCA scores plot. Therefore, reading of both the PCA scores and loadings plots is necessary for correct data interpretations. PC1 explains the largest variation of data sets followed by other PCs explaining remaining data sets variation. A high Eigen value on the scores plot (>2) and loadings plots (>0.2) indicate that the sample and variance are significant. The details of PCA methodology and data interpretation can be found in our previous publications (Esbensen et al. 1994; Haware et al. 2009a, 2009b, 2010).

4.2.1. PCA of deforming materials

A PCA analysis of predominantly plastic (Vivapur® 101) and elastic (Starch 1500®) materials is shown in Figure 4. The first two PCs explained 74% variance in the data. The PCA analysis used five PCs to explain 100% variance in the data. The PCA scores plot (Figure 4(A)) displayed the expected separate grouping of predominantly plastic and elastic materials along the PC1. This confirmed their respective deformation followed by different tableting performances.

Vivapur® 101 showed a negative correlation with the CM and YPpl along the PC1 in the PCA loadings plot (Figure 4(B)). It possibly insinuates the smooth plastic deformation of Vivapur® 101 at the low compression pressure. Vivapur® 101 displayed a positive correlation with decompression modulus, WoC, YPel, and TMS along the PC1. A positive correlation of Vivapur® 101 with decompression modulus and YPel suggesting a requirement of high-pressure of this material for its possible elastic recovery during the unloading of the compression pressure. Such materials could show a limited elastic recovery after the permanent deformation during the compression cycle, which finally translates into a stronger compact formation (Haware et al. 2009a). An expected positive relationship of Vivapur® 101 with WoC confirmed the requirement of a high energy consumption of plastic materials during the compression process (Haware et al. 2010; Bolhuis and Waard 2011).

The predominantly elastic Starch 1500® displayed an opposite trend as that of Vivapur® 101 along the PC1 axis. A positive correlation of Starch 1500® with CM, YPpl and a negative correlation with decompression modulus, YPel, WoC, and the TMS suggest its resistance for the material deformation in the compression phase but readiness for deformation recovery in the decompression phase (Bolhuis and Waard 2011). Such material's elastic nature is known to offer an unfavorable environment for robust tableting (Paronen 1986; Bolhuis and Waard 2011).

4.2.2. PCA of fragmenting materials

As fragmentation occurs at relatively low compression pressures (De Boer et al. 1986), the PCA analysis (Figure 5) of predominantly high (Emcompress®) and low (Tablettose® 100) fragmenting materials was performed with the CDM evaluated at a low-compression pressure range (5–20 MPa). However, the remaining descriptors were evaluated in similar compression conditions like the above-mentioned deforming materials. The first two PCs explained 79% variance in the data. The PCA analysis used five PCs to explain 100% variance in the data. A separate grouping of low fragmenting (Tablettose® 100) and high fragmenting (Emcompress®) materials is observed along the PC2 axis of the

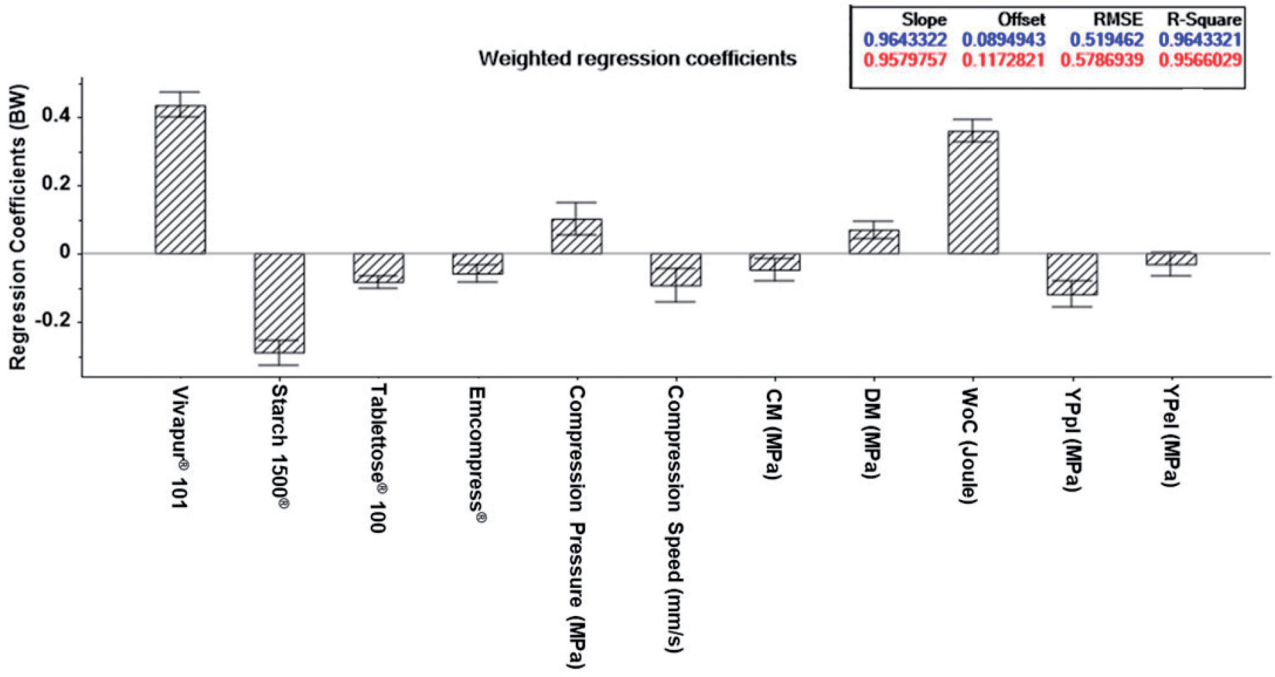

Figure 6. The principal regression analysis plot indicating weighted regression coefficients of main effects of all *X*-variables (material type, compression pressure, compression speed, compression modulus, decompression modulus, work of compression, YPpl, and YPel) on the *Y*-variable (tablet mechanical strength).

PCA scores plot (Figure 5(A)). Similar separation along the PC2 was observed with two microcrystalline celluloses Vivapur® 101 and Avicel® 101 in our previous studies (Haware et al. 2010). It could be due to smaller differences between the material fragmentation, compression characteristics, and tablet properties of these brittle materials. Emcompress® exhibited a positive correlation with the decompression modulus, YPpl, and YPel, and a negative correlation with the CM along the PC2 axis (Figure 5(B)). An exactly opposite trend is observed for Tablettose® 100 along the same axis. A respective negative and positive correlation of Emcompress® and Tablettose® 100 with CM indicates relative softness of Emcompress® as compared to Tablettose® 100. A high material stiffness of Tablettose® 100 is further corroborated by its positive correlation with the WoC along the PC2 axis. Emcompress® also showed a positive correlation with YPpl and YPel. These placements confirm the respective high and low fragmentation capacities of Emcompress® and Tablettose® 100 under the applied compression load. It could insinuate that a high fragmenting soft Emcompress® could form the stronger tablets than a low fragmenting stiff Tablettose® 100. Consequently, six Emcompress® experiments compared to four Tablettose® 100 experiments displayed a positive correlation with TMS along the PC1 axis (Figure 5(A,B)).

4.3. Quantitative analysis between material deformation properties and tablet mechanical strength

A quantitative relationship between evaluated material properties and TMS was assessed with PCR (Figure 6). The *X*-variables of this analysis were material types, compression pressure, compression speed, CDM, WoC, and Heckel's descriptors. The *Y*-variable was TMS. The *X*-variables whose error bar is not passing through the origin are considered as statistically significant variables. The impact of the *X*-variable on the respective *Y*-variable is considered statistically insignificant when its error bar is passing through the origin. The *X*-variables having a positive regression coefficient shows a positive impact on the TMS and vice-a-versa. The bar height in the weighted regression coefficient indicates their low or high statistically significant impact on the *Y*-variable. A model statistical significance was calculated at $\alpha < 0.05$. Further details of PCR modeling will be found elsewhere (Haware et al. 2010). Only the main effects of the variables are evaluated in the present PCR model (Figure 6). The effect of different deforming and fragmenting materials on the TMS was calculated by initially coding them as a 'category variable' and then subsequently splitting the coded category variables. The present model used seven PCs to evaluate the data. The first two PCs explained 49% *X*-variance and 68% *Y*-variance in the data. The regression coefficient (R^2) of an optimized PCR model at the calibration and the validation stage is 0.9643 and 0.9566, respectively. The root mean square error (RMSE) of an optimized PCR model at the calibration and the validation stage is 0.52 MPa, and 0.58 MPa, respectively.

4.3.1. Impact of material types

The PCR model suggests that the formulations dominated with plastically (Vivapur® 101) and elastically (Starch 1500®) deforming materials will exhibit a statistically significant positive and negative impact on the TMS. This relationship was also observed in the qualitative PCA along the PC1 axis. A permanent plastic deformation is known for its stronger bonding due to the increased bonding area between the plasticized particles (Nyström and Karehill 1996; Bolhuis and Waard 2011). This confers the required strength to the formulated tablet. On the other hand, relapsing elastic material deformation is an unfavorable mechanism for particle bonding. The bonding contact area and subsequent bond strength of predominantly elastic materials decrease when deformed particles try to regain their majority of original particle dimensions during or after unloading of the applied compression pressure (Nyström and Karehill 1996). Such elastically behaving materials are known to produce weaker tablets vulnerable to potential capping and lamination issues (Armstrong and Haines-Nutt 1974; Nyström and Karehill 1996).

The model further suggests that the formulations dominated by fragmenting materials will show a statistically significant

negative impact on the TMS. Formulations consisting of low fragmenting materials (Tablettose® 100) will show a significantly higher negative impact on the TMS than high fragmenting materials (Emcompress®). As both materials exhibited a negative impact on the TMS (high vs. low negative impact), they displayed a separate grouping along the PC2 axis in the PCA (Figure 5(A)). The negative impact of the fragmenting materials in the optimized PCR models is statistically less than the negative impact of elastic materials on the TMS. It insinuates the ability of fragmenting materials to form relatively stronger tablets than elastic materials. It is known that the overall bonding strength of the fragmented material is a function of the number of bonds generated after the breakage of individual particles into several sub-particles (De Boer et al. 1986; Haware et al. 2009a).

4.3.2. Impact of compression conditions

The PCR model revealed respective statistically significant negative and positive impacts of the compression speed and compression pressure. The deforming materials are forming weaker tablets at high compression speed. Materials have less time to experience the applied compression pressure at high compression speed and its subsequent translation into the bond favorable material deformation (Roberts and Rowe 1985; Armstrong and Palfrey 1989). This is also called 'strain rate sensitivity'. Fragmenting materials are more immune to the compression speed sensitivity, but as per our finding, fragmenting materials did show sensitivity to the applied compression speed (Haware et al. 2009b). This could explain the statistically negative impact of the compression speed on the TMS. The common materials used in pharmaceutical industry undergo better fragmentation and deformation under the higher compression pressure, which eventually translates into stronger tableting.

4.3.3. Impact of compression and decompression modulus

The CM exhibited a negative impact on the TMS. It insinuates that materials having a low CM could form stronger tablets. A low CM is a property of soft materials. The soft materials are highly compressible due to high inter-planer spacing (*d*-spacing) inside their crystal. The authors are aware that highly compressible soft materials did not necessarily produce stronger tablets (Joshi et al. 2018). However, in the present study, relatively strong bond forming plastic Vivapur® 101 and high fragmenting Emcompress® showed relatively low CM than a weaker bond forming elastic Starch 1500® and a low fragmenting Tablettose® 100, especially in the low compression region. These findings confirm that relatively soft materials with plastic deformation and high fragmenting tendency would be a better choice for stronger tableting than hard materials with elastic deformation and low fragmenting tendency.

The decompression modulus presented a statistically significant positive impact on the TMS. The decompression modulus could be used as an indicator of compact elastic recovery. Materials having a high decompression modulus could show low '*in-die*' compact elasticity during the decompression phase, which clearly suggests preserved deformation and material fragmentation required for the successful inter-particulate bonding survival. Clearly, studied fragmenting materials showed the highest decompression modulus in all materials. This confirms their lowest '*in-die*' elastic recovery. An elastic Starch 1500® exhibited the lowest decompression modulus insinuating its high compact '*in-die*' elastic recovery, which ultimately translated into weaker tablets.

4.3.4. Impact of Heckel and work descriptors

Heckel descriptors such as YPpl and YPel are the indicators of the plasticity and elasticity of the materials, respectively. These Heckel descriptors displayed significantly negative impacts on the TMS in the optimized PCR model. Materials having low YPpl required less pressure to deform plastically. As these materials are ready to deform plastically, they offer stronger bonding strength during the compact formation. On the contrary, fragmenting materials are not readily deformable. They require more compression pressure (high YPpl) than plastic materials for a possible permanent deformation. As mentioned previously, the particle bonding success of fragmenting materials is based on the number of bonds between the fragmented particles rather than the bonding area between the deformed particles (Nyström and Karehill 1996). However, the majority of the plastic materials form stronger bonding as compared to the fragmenting materials. This was also the case in the present study, which is reflected by a statistically significant negative impact of YPpl on the TMS.

A low YPel implies less pressure requirement of a compact for the possible axial elastic recovery after the release of compression pressure. As the majority of the deformation gets recovered easily (low YPel) during the unloading process, such materials are termed as a 'predominantly elastic material'. This can lead to a reduction in the bonding area followed by a bonding strength of the deformed particles. These events eventually translate into the formation of weaker tablets. Due to this, elastic materials are known to form the weaker tablets compared to the fragmenting and plastic materials. This trend was mirrored with a statistically significant negative impact of YPel on the TMS. However, it is important to note that, unlike a decompression modulus, this elastic recovery indicator Heckel descriptor is about to become statistically insignificant though these different parameters are derived from the same compression profile generated under similar experimental settings.

Finally, WoC displays a positive impact on the TMS. A bond favoring particle permanent material deformation and fragmentation are energy-consuming processes. The particle fragmentation and deformation are respective low- and mid-pressure events that occur during the compression phase. Therefore, the energy consumption of plastic deformation is more as compared to fragmentation. Clearly, materials relying on these events seem to exhibit a high WoC with the formation of a stronger compact.

4.4. Compliance of moduli and Heckel descriptors

A present qualitative and quantitative statistical analysis implies complementary nature of the modulus descriptors (CM and DM) to Heckel descriptors (YPpl and YPel) in order to explain material deformation and compact elastic recovery. A quantitative PCR analysis exhibited a statistically significant negative impact of material deformation indicators CM and YPpl on the TMS. Similarly, compact elastic recovery indicators DM and YPel presented a statistically significant negative impact on the TMS. However, DM has a more pronounced effect than YPel as YPel is on the verge of becoming statistically insignificant in the same setting during the data analysis. Additionally, there are certain limitations with the Heckel analysis. The most prominent limitation of the Heckel analysis is a requirement of the powder particle density to calculate the '*in-die*' relative density at applied compression pressure (Patel et al. 2022). A small error (1%) in the density measurement causes a 10% error in the Heckel descriptors calculations (Sonnergaard 1999). The Heckel analysis exhibits a negative porosity issue at very high compression pressures, as

pre-compression particle density is not a real presentation of an '*in-die*' dynamic particle density (Patel et al. 2022). This can hinder the full material and formulation characterization using generated '*in-die*' compression profiles with the compaction simulator. The proposed modulus descriptors (CM and DM) can overcome Heckel analysis limitation, as these measurements do not require the powder particle density measurements. As mentioned earlier, modulus descriptors require only punch displacement and applied compression pressure data to evaluate the material characteristics. Therefore, present statistical similarities between the modulus descriptors (CM and DM) and Heckel descriptors insinuate that the derived moduli could serve as an alternative if not complementary to the Heckel descriptors.

4.5. Proposed material classification system based on compression and decompression modulus

As derived CDM displayed their statistically significant correlation with the TMS in the optimized PCR model, these descriptors were used to propose a new material classification system. This is called as CDMCS. The pharmaceutical materials are classified into four different classes based on their extremely low, low, high, extremely high CDM (Table 1). The CDM derived in low (5–20 MPa) and mid-pressure regions (20–60 MPa) were used to develop this classification system (Figure 7).

The class-I materials have an extremely low compression and a low decompression modulus in both low- and mid-pressure regions. These materials will form a stronger compact. The majority of plastic materials will fall into this category.

The class-II materials have a low compression and an extremely high decompression modulus in the low-pressure range. These materials have an extremely high compression and a high decompression modulus in the mid-pressure range. These materials could form the second strongest compact after the class-I materials. High fragmenting materials will belong to this class.

The class-III materials display a high compression and a high decompression modulus in both low- and mid-pressure ranges. These materials could form weaker tablets than the class-II materials. Low fragmenting materials will fit in this class.

The class-IV materials exhibit an extremely high and a high CM in the low-and mid-pressure range, respectively. These materials possess an extremely low decompression modulus in both pressure ranges. These materials will form extremely weak compacts. Predominantly elastic materials fall in this class. A formulation belonging to class-IV could pose potential tableting problems like capping and lamination.

5. Conclusions

The present investigation demonstrated the application of CDM derived from the dynamic continuous compression profile in the characterization and classification of the deformation behavior of pharmaceutical materials. The CDM exhibited statistically significant negative correlations with the TMS like Heckel YPpl and YPel descriptors. A qualitative PCA and quantitative PCR analysis showed that the statistical significance of moduli descriptors on the TMS was equally and/more prominent than the Heckel descriptors. Importantly, the estimated modulus descriptors are independent of particle density measurements, unlike Heckel descriptors. Thus, these moduli descriptors could serve as an alternative to the Heckel descriptors when the Heckel method fails due to a high-pressure range negative porosity issue. This feature of modulus descriptors is specifically beneficial to utilize the decompression phase profile for estimating formulation elasticity responsible for tableting problems like capping and lamination,

Table 1. Compression–decompression classification range.

	Low compression pressure range (5–20 MPa)		Mid compression pressure range (20–60 MPa)	
Classification	Compression modulus range	Decompression modulus range	Compression modulus range	Decompression modulus range
Extremely low	0–72	0–944	0–284	0–4174
Low	73–98	945–1704	285–354	4175–6315
High	99–107	1705–2206	355–428	6316–10 856
Extremely high	108–151	2207–3491	428–476	10857–15807

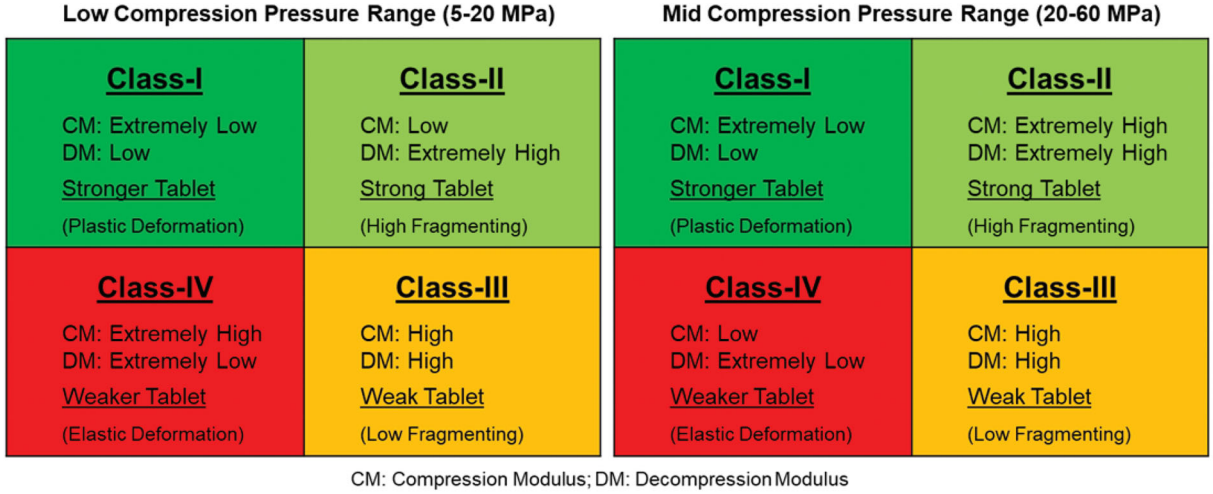

Figure 7. Compression-decompression modulus classification system (CDMCS) for Low (5-20 MPa) and Mid (20-60 MPa) compression pressure ranges. If CM and DM of the material lies in the green (Class-I) or light green (Class-II) region, then the material may result into robust tablets. If CM and DM of the material lies in the orange (Class-III) or red (Class-IV) region, then the material may result into poor tablets.

where the Heckel plot decompression phase is vanishing due to the negative porosity issue. Additionally, a two-dimensional pharmaceutical material classification system is established based on the CDM. The materials with predominantly plastic and high fragmentation tendency are classified as class-I and class-II materials, respectively. A formulation consisting of materials from these classes could produce stronger tablets. Predominantly low fragmenting and elastic materials were placed in class-III and class-IV. A formulation developed with the materials from class-III and class-IV could produce weaker tablets. These formulations might be more prone to tablet capping and lamination. Clearly, though the analysis is based on limited model materials data, the proposed compression behavior parameterization methodology and classification system could serve as a 'first-hand tool' in an early formulation development stage or as a 'tableting problem diagnostic tool' in the late development stage.

Disclosure statement

No potential conflict of interest was reported by the author(s).

Funding

The author(s) reported there is no funding associated with the work featured in this article.

References

Akseli I, Hancock BC, Cetinkaya C. 2009. Non-destructive determination of anisotropic mechanical properties of pharmaceutical solid dosage forms. Int J Pharm. 377(1–2):35–44.

Armstrong NA, Palfrey LP. 1989. The effect of machine speed on the consolidation of four directly compressible tablet diluents. J Pharm Pharmacol. 41(3):149–151.

Armstrong NA, Haines-Nutt RF. 1974. Elastic recovery and surface area changes in compacted powder systems. Powder Technol. 9(5–6):287–290.

Bolhuis GK, Waard Hd. 2011. Compaction properties of directly compressible materials. In: Çelik M, editor. Pharmaceutical powder compaction technology. 2nd ed. New York: Marcel Dekker, Inc.; p. 143–204.

Çelik M, Okutgen E. 1993. A feasibility study for the development of a prospective compaction functionality test and the establishment of a compaction data bank. Drug Dev Ind Pharm. 19(17–18):2309–2334.

Choi DH, Kim NA, Rok CH, Jung JY, Yoon J-H, Jeong SH. 2010. Material properties and compressibility using Heckel and Kawakita equation with commonly used pharmaceutical excipients. J Pharm Investig. 40(4):237–244.

David ST, Augsburger LL. 1977. Plastic flow during compression of directly compressible fillers and its effect on tablet strength. J Pharm Sci. 66(2):155–159.

De Boer AH, Vromans H, Leur CF, Bolhuis GK, Kussendrager KD, Bosch H. 1986. Studies on tableting properties of lactose. Part III. The consolidation behaviour of sieve fractions of crystalline α-lactose monohydrate. Pharm Weekbl Sci. 8(2):145–150.

Esbensen K, Schönkopf S, Midtgaard T, Guyot D. 1994. Multivariate analysis in practice. Trondheim, Norway: CAMO ASA.

Fell JT, Newton JM. 1970. Determination of tablet strength by the diametral-compression test. J Pharm Sci. 59(5):688–691.

Haware RV, Bauer-Brandl A, Tho I. 2010. Comparative evaluation of the powder and compression properties of various grades and brands of microcrystalline cellulose by multivariate methods. Pharm Dev Technol. 15(4):394–404.

Haware RV, Tho I, Bauer-Brandl A. 2009a. Application of multivariate methods to compression behavior evaluation of directly compressible materials. Eur J Pharm Biopharm. 72(1):148–155.

Haware RV, Tho I, Bauer-Brandl A. 2009b. Multivariate analysis of relationships between material properties, process parameters and tablet tensile strength for α-lactose monohydrates. Eur J Pharm Biopharm. 73(3):424–431.

Haware RV, Tho I, Bauer-Brandl A. 2010. Evaluation of a rapid approximation method for the elastic recovery of tablets. Powder Technol. 202(1–3):71–77.

Heckel RW. 1961a. An analysis of powder compaction phenomena. Trans Metall Soc AIME. 221:1001–1008.

Heckel RW. 1961b. Density–pressure relationships in powder compaction. Trans Metall Soc AIME. 221:671–675.

Joshi TV, Singaraju AB, Shah HS, Morris KR, Stevens LL, Haware RV. 2018. Structure-mechanics and compressibility profile study of flufenamic acid: nicotinamide cocrystal. Cryst Growth Des. 18(10):5853–5865.

Martens H, Martens M. 2000. Modified Jack-knife estimation of parameter uncertainty in bilinear modelling by partial least squares regression (PLSR). Food Qual Prefer. 11(1–2):5–16.

Nyström C, Karehill P-G. 1996. The importance of intermolecular bonding forces and the concept of bonding surface area. In: Alderborn G, Nyström C, editors. Pharmaceutical powder compaction technology, 1st ed. New York: Marcel Dekker, Inc.; p. 17–53.

Paronen P. 1986. Heckel plots as indicators of elastic properties of pharmaceuticals. Drug Dev Ind Pharm. 12(11–13):1903–1912.

Patel DB, Patel VD, Haware R, Sedlock R. 2022. Negative porosity issue in the Heckel analysis: a possible solution; In communication.

Ragnarsson G. 1996. Force–displacement and network measurements. In: Alderborn G, Nyström C, editors. Pharmaceutical powder compaction technology, 1st ed. Vol. 71. New York: Marcel Dekker, Inc.; p. 80–81.

Roberts RJ, Rowe RC. 1985. The effect of punch velocity on the compaction of a variety of materials. J Pharm Pharmacol. 37(6): 377–384.

Rue PJ, Rees JE. 1978. Limitations of the Heckel relation for predicting powder compaction mechanisms. J Pharm Pharmacol. 30(10):642–643.

Sonnergaard JM. 1999. A critical evaluation of the Heckel equation. Int J Pharm. 193(1):63–71.